Article No. mb981920 J. Mol. Biol. (1998) 281, 95–106

JMB

Two Antibodies that Neutralize Papillomavirus by Different Mechanisms Show Distinct Binding Patterns at 13 Å Resolution

Frank P. Booy[1], Richard B. S. Roden[2], Heather L. Greenstone[2] John T. Schiller[2] and Benes L. Trus[1,3]*

[1]*Laboratory of Structural Biology, National Institute of Arthritis and Musculoskeletal and Skin Diseases, National Institutes of Health, Bethesda MD 20892, USA*

[2]*Laboratory of Cellular Oncology, National Cancer Institute, National Institutes of Health, Bethesda MD 20892, USA*

[3]*Computational Bioscience and Engineering Laboratory Division of Computer Research and Technology, National Institutes of Health, Bethesda MD 20892, USA*

**Corresponding author*

Complexes between bovine papillomavirus type 1 (BPV1) and examples of two sets of neutralizing, monoclonal antibodies (mAb) to the major capsid protein (L1) were analyzed by low-dose cryo-electron microscopy and three-dimensional (3D) image reconstruction to 13 Å resolution. mAb #9 is representative of a set of neutralizing antibodies that can inhibit viral binding to the cell surface, while mAb 5B6 is representative of a second set that efficiently neutralizes papillomaviruses without significantly inhibiting viral binding to the cell surface. The 3D reconstructions reveal that mAb #9 binds to L1 molecules of both pentavalent and hexavalent capsomeres. In contrast, 5B6 binds only to hexavalent capsomeres, reflecting the significant structural or environmental differences for the 5B6 epitope in the 12 pentavalent capsomeres. Epitope localization shows that mAb #9 binds monovalently to the tips of capsomeres whereas 5B6 binds both monovalently and bivalently to the sides of hexavalent capsomeres approximately two-thirds of the way down from the outer tips, very close to the putative stabilizing intercapsomere connections. The absence of mAb 5B6 from the pentavalent capsomeres and its inability to prevent viral binding to the cell surface suggest that receptor binding may occur at one or more of the 12 virion vertices.

© 1998 Academic Press

Keywords: papillomavirus; cryo-electron microscopy; neutralizing antibodies; 3D structure; image reconstruction

Introduction

Papillomavirus infections typically produce benign epithelial papillomas, or warts, but a subset of human (HPV) types is associated with a number of human malignancies, most commonly cervical cancer (International Agency for Research on Cancer, 1995; Lowy *et al*., 1994). Over 90% of cervical cancers are associated with HPV infection and cervical cancer is the second leading cause of death from cancer in women worldwide. Since genital human papillomavirus infection is generally sexually transmitted, considerable effort has been devoted to the development of a prophylactic vaccine for administration to adolescents. In principle, this vaccine would prevent infection by inducing the generation of neutralizing antibodies (Schiller & Okun, 1996).

The 600 Å diameter papillomavirus consists of a histone-bound 8 kb double-stranded, cccDNA (covalently closed circular) genome core encapsidated by a non-enveloped icosahedral shell comprising a major (L1) and a minor (L2) capsid protein in a ratio of approximately 30:1 (Pfister, 1987). The inability to generate preparative quantities of papillomaviruses *in vitro* has prevented an X-ray crystallographic analysis of virion structure (Hagensee & Galloway, 1993). However, sufficient virions have been purified from warts for cryo-electron microscopy (Baker *et al*., 1991; Belnap *et al*., 1996; Trus *et al*., 1997). Using Cross Common Lines procedures (Baker *et al*., 1988; Crowther, 1971;

Abbreviations used: BPV1, bovine papillomavirus type 1; mAb, monoclonal antibodies; L1, major capsid proteins; L2, minor capsid protein; 3D, three-dimensional; kb, kilo base-pairs; cccDNA, covalently closed circular DNA; CRPV, cottontail rabbit papillomavirus; VLP, virus-like particle; IgG, immunoglobulin G; CTF, contrast transfer function; RHDV, rabbit haemorrhagic disease virus.

E-mail address of the corresponding author: trus@ipalph.dcrt.nih.gov

0022–2836/98/310095–12 $30.00/0 © 1998 Academic Press

Fuller, 1987) and the more recent Polar Fourier Transform methods (Baker & Cheng, 1996) the 3D structures of many viruses and virus–antibody complexes have been determined by cryo-electron microscopy (Hewat & Blaas, 1996; Smith *et al*., 1993a,b; Thouvenin *et al*., 1997; Trus *et al*., 1992). These techniques have been applied to BPV1, HPV1 and cottontail rabbit papillomavirus (CRPV) virions, which all exhibit very similar structures at 25 to 30 Å resolution (Baker *et al*., 1991; Belnap *et al*., 1996). Image reconstructions of papillomaviruses show prominent pentameric star-shaped capsomeres that are arranged into $T = 7$ icosahedral capsids (Baker *et al*., 1991; Belnap *et al*., 1996; Hagensee *et al*., 1994). Since very similar icosahedral virus-like particles (VLPs) can be generated by L1 molecules alone (Hagensee *et al*., 1994; Kirnbauer *et al*., 1992), assembled L1 molecules must be versatile enough to coordinate different numbers of capsomeres; each of the 60 hexavalent capomeres per capsid is coordinated with six capsomeres, whereas each of the 12 pentavalent capsomeres (located at the vertices of the icosahedron) is surrounded by five neighbouring capsomeres (Belnap *et al*., 1996).

The location of L2 within the capsid was not determined by comparison of 3D reconstructions of HPV1 L1 and L1/L2 VLP structures, possibly due to low resolution (~35 Å) or low L2 occupancy (Hagensee *et al*., 1994). However, a recent study of BPV to 9 Å suggests that L2 may be located at the 5-fold vertices, in the center of the pentavalent capsomeres (Trus *et al*., 1997).

L1 VLPs retain the neutralizing epitopes of the virus but do not contain the potentially oncogenic viral genome (Kirnbauer *et al*., 1992; Schiller & Roden, 1996). Immunization of animals with VLPs induces high titers of type-specific neutralizing antibodies to epitopes on L1 (reviewed by Schiller & Roden, 1996). Furthermore, immunization of animals with VLPs derived from animal papillomaviruses protects them from experimental challenge by the cognate infectious virions (Breitburd *et al*., 1995; Kirnbauer *et al*., 1996; Suzich *et al*., 1995). Passive transfer experiments demonstrate that this protection can be mediated by neutralizing serum immunoglobulin gamma (IgG) (Breitburd *et al*., 1995; Suzich *et al*., 1995). These properties make VLPs attractive candidates for a prophylactic vaccine against high-risk genital HPV infection and have prompted a study of the mechanism of papillomavirus neutralization by IgG molecules (Schiller & Roden, 1996).

Analysis of mAbs to papillomaviruses demonstrates that neutralization for the types tested, including BPV1, CRPV, HPV11, and HPV16, can occur by more than one mechanism (Christensen & Kreider, 1991, 1993; Christensen *et al*., 1990; Roden *et al*., 1994, 1996). One set of neutralizing mAb to L1, typified by mAb #9 to BPV1 L1, can prevent virions from binding to cell surfaces (Roden *et al*., 1994, 1995), presumably by blocking interaction with a cell surface receptor, which may be α_6 integrin (Evander *et al*., 1997). A second set of neutralizing antibodies to L1, of which 5B6 to BPV1 L1 is an example, does not significantly inhibit virions binding to cell surfaces, yet efficiently prevents infection. For both antibodies, neutralization is achieved with relatively few antibodies bound per virion, although significantly more antibody molecules are required for mAb #9 than for 5B6 (Table 1).

These neutralizing antibodies bind to conformationally dependent and papillomavirus type-specific epitopes on L1, whose amino acid composition and location on the capsid surface are unknown. In order to gain insight into the location of the neutralizing epitopes and the mechanisms of virion neutralization, we have generated the first 3D image reconstructions of papillomavirus–neutralizing antibody complexes: BPV1 virions complexed with saturating amounts of mAb #9 or 5B6.

Results

Figure 1A shows a cryo-electron micrograph of BPV1 purified from cattle warts. The characteristic icosahedral nature and, in certain orientations, some protruding capsomeres of the capsid can be

Table 1. Properties of mAbs #9 and 5B6

Property/mAb	mAb #9	5B6
Isotype	IgG 2a(κ)	IgG 2b(κ)
Neutralizes BPV1	Yes	Yes
Capsid protein bound	L1	L1
Conformational epitope	Yes	Yes
Type-specific	Yes	Yes
Binding to RBCs	Inhibits	No inhibition
Binding somatic cells	Inhibits	>50% inhibition
Ab/virion for 50% neutralization	36	14
Location of epitope on capsomere	Tips of all capsomeres	Sides of hexavalent capsomeres
Binds pentavalent capsomeres	Yes (5/5 L1)	No
Binds hexavalent capsomeres	Yes (3/5 L1 with high occupancy)	Yes (5/5 L1)
Antibody binding	Monovalent	Bivalent and monovalent
High occupancy epitopes per virion	240	300
Number of IgGs bound per virion	240	150

These data are summarized from Roden *et al*. (1994) and this manuscript

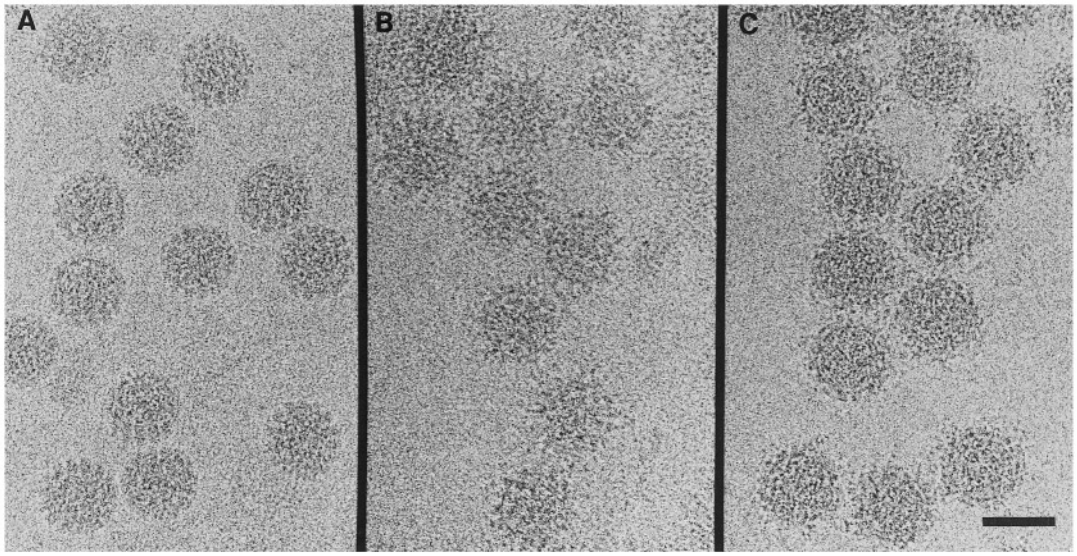

Figure 1. Cryo-electron micrographs of: A, native BPV1 virions; B, BPV1 complexed with mAb #9; and C, BPV1 labeled with mAb 5B6. Bar represents 500 Å.

seen, but otherwise few features can be discerned. A small percentage (~1%) of the particles had lower density cores, indicative of capsids lacking the viral genome (not shown). Figure 1B and C shows BPV1 bound to saturating amounts of mAb #9 and 5B6, respectively. Both antibodies obscure the capsomeric structures and the antibody–virion complexes have a greater diameter than virions alone. mAb #9 and, to a lesser extent, mAb 5B6 induced aggregation of the virus.

Micrographs, selected on the basis of their visual appearance and optical diffraction pattern, were digitized at a sampling rate of 2.9 to 4.3 Å/pixel. The orientation and origin of each particle was then determined and refined to enable the calculation of the 3D structure using established procedures (Crowther, 1971; Trus *et al*., 1997).

Reconstruction of BPV complexed with mAb #9

A reconstruction of BPV1 bound by neutralizing mAb #9, calculated to a resolution of 13 Å from 178 contrast transfer function (CTF) corrected images combined from two micrographs, is shown as a surface shaded view along its 2-fold axis in stereo (Figure 2b) and its 5-fold axis (Figure 3c). A previously described (Trus *et al*., 1997) reconstruction of native BPV1 viewed down the 2-fold axis in stereo (Figure 2a) and the 5-fold axis (Figure 3) is shown at 13 Å resolution for comparison with the antibody-decorated capsids. Although the complete mAb #9 IgG was used to bind BPV1, only part of the mAb is visible in the reconstruction for the following reasons: firstly, although the F_{ab} regions of mAb #9 are bound to the capsid and are ordered with icosahedral symmetry, the unbound F_{ab} and F_c portions may be flexible enough to take up multiple orientations, resulting in blurring of protein density with increasing radius (Smith *et al*., 1993a); secondly, it was necessary to window the 2D input images at a radius of 348 Å because of the close proximity of neighboring particles (probably resulting from mAb #9 cross-linking the virus particles). Thus any F_c or F_{ab} domains would not be visualized beyond this radius. A lower-resolution reconstruction (25 Å) was also calculated from a subset of the particles that could be windowed at a larger radius (380 Å) to visualize the F_c or F_{ab} domains better (data not shown). Inter-capsomere cross-linking of the virus by two F_{ab} fragments was not observed up to the maximum radius investigated.

In Figure 4d, five F_{ab} fragments are bound to the pentavalent capsomeres, demonstrating that the vertex capsomeres in papillomaviruses contain five L1 molecules, each displaying an epitope for mAb #9. This mAb also binds to hexavalent capsomeres but to only three of the five constituent L1 molecules with a sufficient degree of occupancy to be visualized clearly (Figure 4c). Examination of serial sections (data not shown) demonstrated that the protein density at 1 o'clock above the hexavalent capsomere is actually connected to the IgG bound to the pentavalent capsomer and simply overhangs the hexavalent capsomer as seen. Thus there is a potential for 240 sites per virion to bind F_{ab} fragments of mAb #9 (out of a total of 360 L1 molecules) with high occupancy.

In the central cross-section shown in Figure 5b (cut vertically as indicated in Figure 2a to pass through the 2-fold, 5-fold and 3-fold axes, with the central 2-fold axis of Figure 2 appearing at the 12 o'clock position in Figure 5), it is evident that the mAb #9 F_{ab} fragments bind to the tips of the capsomeres. The cross-section of our previously described (Trus *et al*., 1997) native BPV1 virion reconstruction is shown for comparison (Figure 5a) at the same resolution. At the 5-fold axis the mAbs extend radially outwards for ~35 Å before leaving this section (see also the

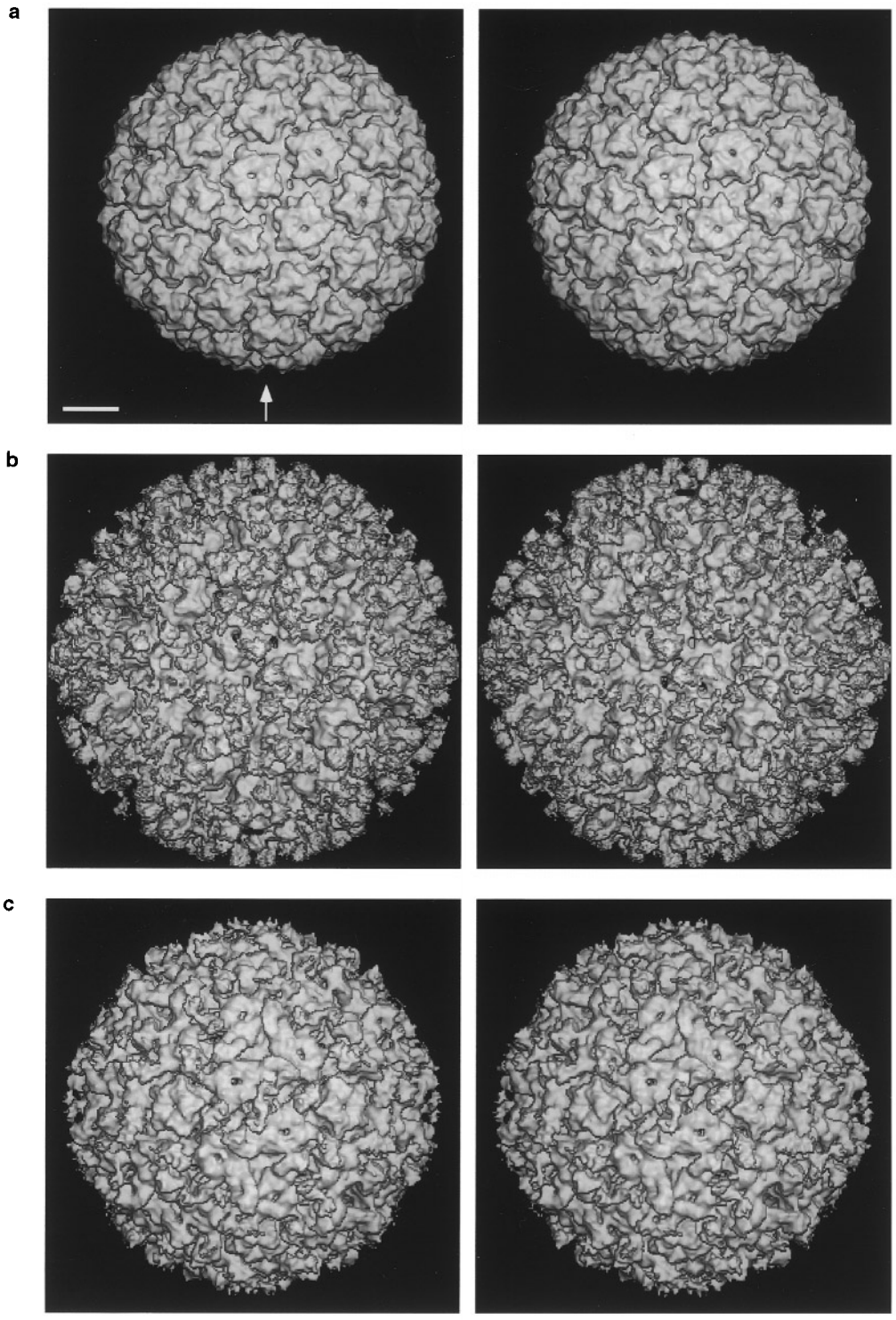

Figure 2. Surface-shaded, stereo views down the 2-fold axis of symmetry of 3D reconstructions at 13 Å resolution of: a, BPV1; b, BPV1 labeled with mAb #9; and c, BPV1 labeled with mAb 5B6. a, Taken from a previously described reconstruction (Trus *et al.*, 1997), but the data are truncated at 13 Å resolution. The arrow in a indicates the location of the cross-section visualized in Figure 5. Bar represents 100 Å.

schematic diagram in Figure 6(b)). The mAb bound to the 2-fold axis (12 o'clock position) extends at about 30° and then bends 120° to form a double arrowhead above the capsid surface, which cannot be seen in the perpendicular 2-fold view (Figure 5b, 9 o'clock position).

Epitope localization of mAb #9

Examination of density sections cut in various orientations and comparison with similar sections from the native BPV structure permit the size and shape of the proximal portions of the mAbs to be

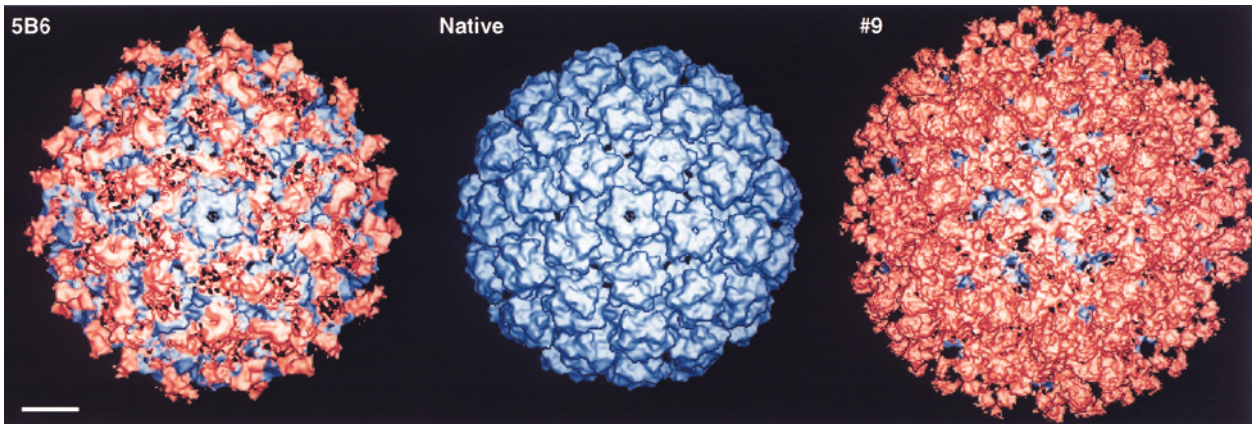

Figure 3. Difference map between the mAb–virion complex and the native virion structures viewed down a 5-fold axis of symmetry. The protein density maps of the reconstructions of the virion alone (native) and the antibody–virion complexes were aligned and a difference map was generated. The density due to mAb is shown in red and the density of BPV1 alone is shown in blue. Bar represents 100 Å.

estimated and the localization of the epitopes to be determined (Figure 7). Spherical sections cut perpendicularly to the 2-fold axis localize the epitope for mAb #9 to sections at a radius of ~295 Å between the protrusions of density comprising the very tip of the capsomeres (Figure 7b).

Reconstruction of BPV complexed with 5B6

The 3D reconstruction of mAb 5B6 complexed with BPV1, generated from 207 images, was also determined to 13 Å resolution. The salient features of this complex are clearly visible in the reconstruction of mAb 5B6 bound to BPV1 viewed in stereo down the 2-fold axis (Figure 2c) and the 5-fold axis (Figure 3). Only a portion of the 5B6 mAb is visualized, as illustrated in Figure 6a. The central section (Figure 5c) appears to show a cross at the hexavalent capsomere on the 2-fold axis (12 o'clock position). No antibody is seen bound to the 5-fold pentamer, contrary to the case for mAb #9.

Epitope localization of mAb 5B6

The epitope for mAb 5B6 can be localized in sections cut perpendicularly to the 2-fold view (Figure 7d) at a radius of 260 to 265 Å. The epitope for 5B6 is visible on the side of the capsomere about 25 Å above the capsid floor. This is very close to the location of the putative C-terminal crosslinks previously reported for BPV (Trus *et al.*, 1997).

As viewed from above, on the 2-fold axis in the surface shaded view (Figure 2c) mAb 5B6 has a well-defined S shape. It is this epitope that is sectioned in Figure 5c at the 12 o'clock position where the Ab seems to form an X. Since the epitopes on the 2-fold axis are only 27 Å apart (Figure 7d), bivalent binding cannot occur. Thus opposing epitopes are probably occupied by a single F_{ab} arm. Consistent with this interpretation, the density of the antibody arms is about half the viral protein density (Figure 5c) while at the point where the antibody arms from the epitopes overlap, the combined density is about the same as the viral protein density. Therefore, the maximum possible occupancy is 50%. Similar binding has been reported before for Ab bound to VLPs derived from the rabbit haemorrhagic disease virus (RHDV) VLPs (Thouvenin *et al.*, 1997).

Other epitopes going counter-clockwise around the non-5-fold (hexavalent) pentamer from the S-shaped Ab are separated by curvilinear distances (measured in a single plane) of 68, 60, 57 and 50(±5) Å, respectively. The closet bivalent spanning distance reported in the literature is 60 Å (Hewat & Blaas, 1996). Therefore, there may be sufficient room for bivalent cross-linking to occur in at least two of these sites. This is supported by the fact that the antibody density linking the epitopes is of a similar magnitude to the density of the viral capsid protein.

mAb 5B6 does not bind to pentavalent capsomeres. The absence of binding to pentavalent capsomeres may be due to steric hinderance, resulting from the close proximity of the potential epitope at the point of the pentavalent capsomere to the point of the adjacent hexavalent capsomere. For the hexavalent capsomere the point of each capsomere faces the wall rather than the point of each surrounding capsomere thus providing sufficient space for antibody binding. mAb 5B6 binds with high occupancy to each of the 300 sites on hexavalent capsomeres.

Visualization of antibody domains

The contorted shape observed for mAb #9 is clearly seen in the stereo pairs shown in Figure 4c and d and in the section shown in Figure 5b. One domain of the Ab entirely covers the top of the star that forms the pentavalent capsomer tip, leaving only the central hole free. Another domain projects away from the first at about 120° into the space between the capsomeres and a third domain pro-

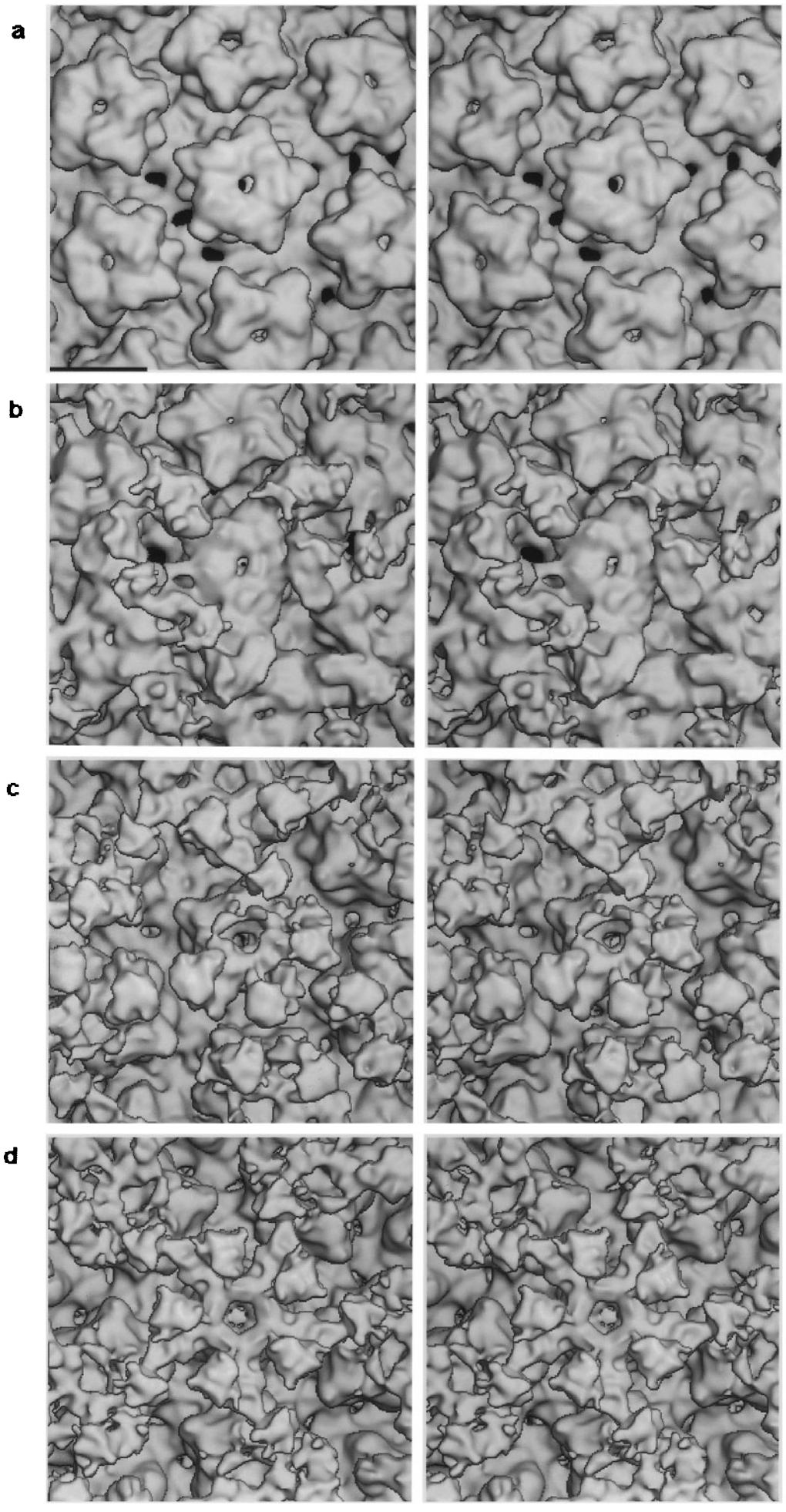

Figure 4 (*legend opposite*)

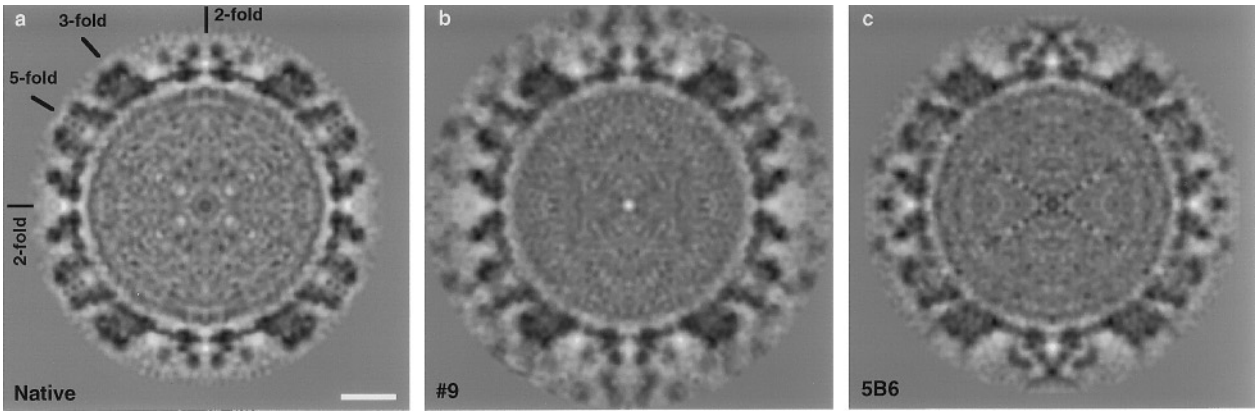

Figure 5. Central density sections (2.6 Å thick) cut through a 2-fold axis of symmetry at 13 Å resolution. a, BPV1; b, BPV1 labeled with mAb #9; and c, BPV1 labeled with mAb 5B6. Protein is in black. Bar represents 100 Å.

jects radially outwards from the intercapsomere space at the side of the second domain. This is shown schematically in Figure 6b where it is proposed that one complete F_{ab} and part of the second F_{ab} and F_c domains are visualized. Since substantial inter-virus crosslinking was observed, it is likely to be the second F_{ab} arm that projects radially outwards and the F_c that overhangs the adjacent hexavalent capsomere, sterically limiting its occupancy. Note the extreme flexibility of the elbow and hinge regions required of mAb #9 with no visible distortion of the virus structure itself (see below). Although the Ab fragments from adjacent capsomeres are in close proximity to one another they radiate outwards from the intra-capsomere regions without joining. This is consistent with monovalent binding of mAb #9 immunoglobulin.

In contrast, the 5B6 F_{ab}s appear to adopt a much more linear conformation, binding deeply between hexavalent capsomeres, and apparently occupying all the available space between the capsomeres around the epitope (Figures 4b and 7d). Neither the pentavalent capsomeres nor the tips of the hexavalent capsomeres are decorated. The radial distance from the epitope on the capsomere to the reconstruction cut-off at 317 Å is approximately 70 Å so it is probable that we are visualizing the entire F_{ab} and a small portion of the F_c fragment. X-ray structure determination suggests that in a linear conformation, an F_{ab} fragment is about 80 Å long (Liu *et al.*, 1994). We have also calculated a lower resolution (20 Å) reconstruction from a subset of particles with a radial cutoff at 343 Å, which allows us to visualize a larger portion (~24 Å) of the F_c fragment (data not shown).

To examine if binding of mAb #9 or 5B6 induced a significant conformational change in the BPV capsid, the protein density maps of the reconstructed virion alone and each antibody–virion complex were aligned and a difference map was generated. In Figure 3, the densities unique to the antibody-virus complex are shown in red and the densities of the native virus are shown in blue. mAb 5B6 binds only to the hexavalent capsomeres leaving the vertices of the capsid uncovered. mAb #9, on the other hand, effectively covers the entire capsid. There is no evidence that binding either mAb #9 or 5B6 induces significant change in the virus structure visualized at 13 Å resolution.

Discussion

High-resolution, 3D image reconstructions of low-dose cryo-electron micrographs of BPV1 complexed with two monoclonal antibodies, mAb #9 and 5B6, demonstrate that these antibodies bind to the capsid very differently. These two mAbs also have different properties and mechanisms of neutralization (summarized in Table 1). mAb #9 prevents BPV1 virions from binding to cell surfaces (Roden *et al.*, 1994, 1995). The extensive coverage of the capsid by this antibody and stoichiometric binding of pentavalent capsomeres (see below) suggests that is might neutralize by sterically hindering interaction of the virion with the putative cell surface receptor (Evander *et al.*, 1997; Outlaw & Dimmock, 1991). Since mAb #9 binds monovalently, it might also neutralize by aggregation of the virus, thereby preventing efficient cell-binding or appropriate uptake (Outlaw & Dimmock, 1991).

However, neutralization by mAb #9 may also occur by a post-binding mechanism as mAb #9 will neutralize even after BPV1 has been bound to the surface of mouse C127 cells for four hours at 37°C (unpublished results). Similar data have been obtained for another mAb, B1.A1 (Christensen & Kreider, 1993), with similar properties to mAb #9,

Figure 4. Surface-shaded, stereo views at 13 Å resolution of a hexavalent capsomere of: a, BPV1; b, BPV1 labeled with mAb 5B6; c, BPV1 labeled with mAb #9; and d, a pentavalent capsomere of BPV1 labeled with mAb #9. Bar represents 100 Å.

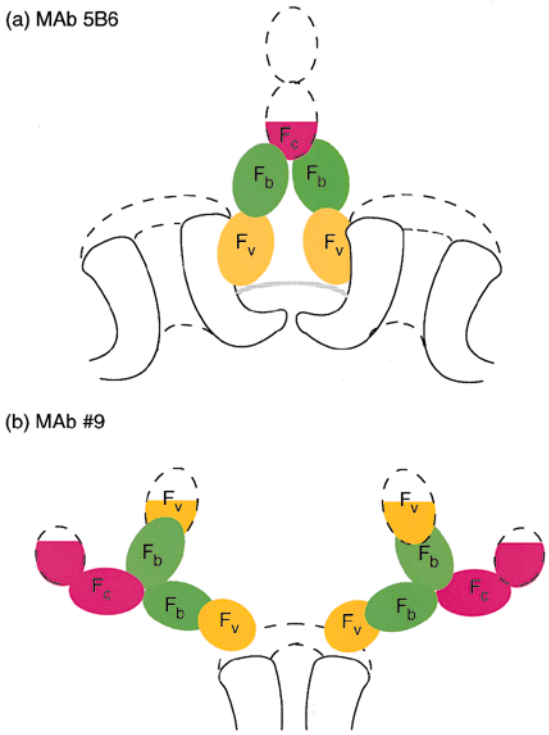

Figure 6. Schematic diagram showing BPV–mAb binding: (a) mAb 5B6 bound between hexavalent capsomeres, just above intercapsomere cross-bridge (indicated as a gray line between the capsomeres); (b) mAb #9 bound to the outer surface, between the points of the pentavalent capsomere.

i.e. it also neutralizes BPV1 and inhibits its binding to cell surfaces (Christensen *et al.*, 1995; Roden *et al.*, 1996). mAbs 5B6, CRPV-5A (Christensen & Kreider, 1991) and H11.B2 (Christensen & Kreider, 1990), which neutralize BPV, CRPV and HPV11, respectively, do not prevent binding of these capsids to erythrocytes (Roden *et al.*, 1996), but also neutralize after virion binding to the cell surface (Christensen *et al.*, 1995). Perhaps there are two receptors for BPV1: a widely expressed and evolutionarily conserved primary receptor and a secondary receptor required during uptake, as seen for adenovirus (Wickham *et al.*, 1993), human immunodeficiency virus-1 (Feng *et al.*, 1996), and herpes simplex virus-1 (Montgomery *et al.*, 1996). Perhaps mAb #9 neutralizes by blocking interaction with both receptors whereas mAb 5B6 only prevents interaction with the secondary receptor.

mAb 5B6 is representative of a second set of neutralizing antibodies that prevents infection without significantly inhibiting virion binding to cell surfaces (Roden *et al.*, 1994, 1995). 5B6 binds between the capsomeres, cross-linking the capsid between at least two pairs of epitopes. The ability to cross-link the capsid suggests that 5B6 might neutralize the virions by preventing the capsid from uncoating and thus releasing the viral DNA into the nucleus, as reported for picornaviruses (Mosser *et al.*,1989; Wetz, 1993). However, bivalent binding is not a prerequisite for neutralization (Colonno *et al.*, 1989). Neutralizing mAb 8F5 to rhinovirus binds in a similar fashion to 5B6 and a similar mechanism of neutralization has been proposed (Hewat & Blaas, 1996).

It is interesting that mAb 5B6 binds close to the putative inter-capsomere linkages. These linkages are thought to help stabilize the capsomere structures against the symmetry mismatch that results from five L1 molecules (which form a hexavalent capsomere) coordinating six surrounding capsomeres. Doubtless, further protein binding close to this region combined with the F_{ab} fragment tightly fitting into the space between the capsomeres further strengthens the structure.

Additional intracellular mechanisms of neutralization such as the re-routing of antibody-bound virions to a non-infectious pathway (e.g. to the lysosomes) cannot be ruled out. In agreement with results from rhinovirus (Hewat & Blaas, 1996; Smith *et al.*, 1993a), no significant changes in capsid morphology were observed between native BPV1 and antibody-coated BPV1 (Figure 3). This suggests that these mAbs do not neutralize by inducing gross conformational changes in virion structure, as has been suggested for poliovirus (Emini *et al.*, 1983).

5B6 binds to each of the L1 molecules in the hexavalent capsomeres, yet to none of the L1 molecules in the pentavalent capsomeres. This may be due to one or more of the following factors: the close apposition of the tips of the pentavalent capsomeres to the tips of the surrounding hexavalent capsomeres, which could sterically hinder antibody binding; conformational differences resulting from the different coordination of the pentavalent and hexavalent capsomeres; and there is the possibility that the presence of L2 in the pentavalent capsomeres precludes Ab binding. A similar difference in antibody binding to pentavalent and hexavalent capsomeres has been observed for the $T = 16$ herpes simplex virus (Trus *et al.*, 1992), although in this case the hexavalent capsomeres do indeed comprise six subunits of the major capsid protein VP5 and the VP26 protein bound at the tip.

The occupancy with which mAb #9 binds to the hexavalent capsomeres (Figure 4c) is noteworthy. There is a clear gradation in occupancy around the hexavalent capsomere in a counter-clockwise direction. One epitope (at the 7 o'clock position in Figure 4c) has high antibody occupancy, close to that seen for the pentavalent capsomeres, and then the occupancy is gradually and significantly reduced until the last two epitopes have very low occupancy. It is probable that this mAb has a higher binding affinity for pentavalent capsomeres and that steric hindrance prevents binding to the two adjacent L1 molecules of the hexavalent capsomere that exhibit very low antibody occupancy. As explained earlier, the protein density overhanging the hexavalent capsomer (1 o'clock position, Figure 4d) is attached to the IgG bound to the pentavalent capsomere and is probably part of the F_c

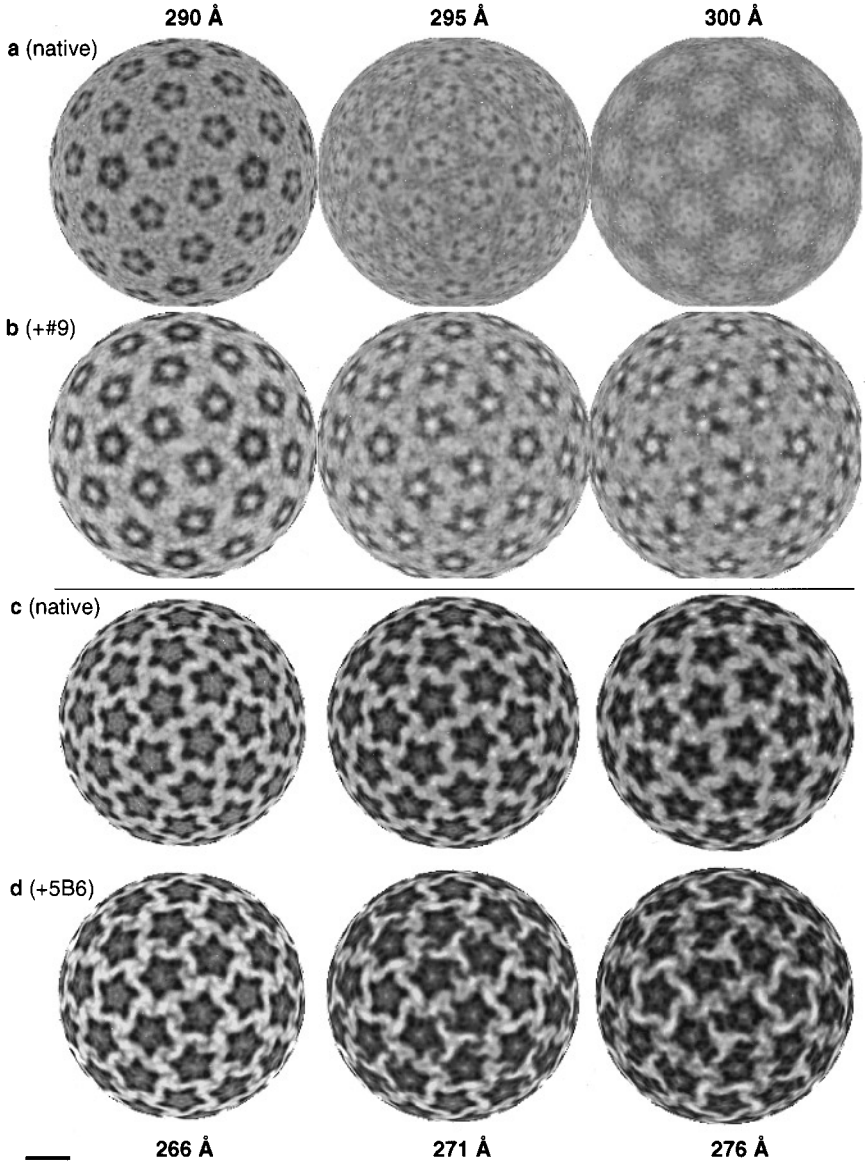

Figure 7. Epitope localization in spherical density sections cut at the radii indicated perpendicularly to the 2-fold axis of symmetry. The sections are 2.6 Å thick. a, native BPV; b, BPV bound with mAb #9; c, native BPV; d, BPV bound with mAb 5B6. Bar represents 100 Å.

fragment (Figure 6b). Flexibility of the Ab domains makes it likely that there is even more unresolved protein sterically hindering binding to the epitopes on the hexavalent capsomere.

Even at 13 Å resolution it was not possible to determine unambiguously the domainal organization of the bound antibodies. In particular, it remains unclear how much of the IgG has been visualized in each of the reconstructions. Some smearing and loss of visibility results from the flexibility of the unbound domains. Nonetheless, the F_{ab} domains assume defined shapes and considerable surface detail is resolved. We propose that the Abs are arranged as depicted in Figure 6 with a significant part of even the F_c portions visualized. This is the first time that these domains have been visualized in an antibody–virion reconstruction. This may reflect the crowded binding by the many mAb #9 IgG molecules per virion reducing the flexibility of the F_c and thus improving its visibility by 3D reconstruction. That more IgG molecules of mAb #9 than 5B6 bind per virion can be seen in Figure 3 and is consistent with the greater concentration of mAb #9 than of 5B6 required for neutralization (see Table 1 and Roden *et al.*, 1994).

The site on papillomavirus capsids that interacts with their cell surface receptor has not been determined. The ability of BPV1 to bind to cell surfaces despite being coated with 5B6 suggests that the cell surface receptor (Evander *et al.*, 1997) is able to bind to areas of the capsid not covered by this antibody (Hewat & Blaas, 1996; Outlaw & Dimmock, 1991). 5B6 binds to hexavalent but not pentavalent capsomeres, thereby leaving the vertices free of

antibody. This suggests that binding site(s) for the cell surface receptor may be located at the vertices. However, it does not preclude the presence of additional binding sites on hexavalent capsomeres as seen for polyomavirus (Stehle *et al*., 1994). In this regard it is worth noting that 5B6 does not obscure the central portion of the hexavalent capsomeres. However, the 5B6 reconstruction does make it unlikely that the cell surface receptor binds in the ''canyon'' between the hexavalent capsomeres, by analogy to the previous proposals for rhinoviruses (Olson *et al*., 1993; Rossmann *et al*., 1985).

These data are the highest resolution 3D reconstructions of virion–mAb complexes to date. Recent advances in cryo–electron microscopy and 3D reconstruction techniques have allowed visualization of protein secondary structure and now even the polypeptide chain (Böttcher *et al*., 1997; Conway *et al*., 1997; Trus *et al*., 1997). In the near future, it may be possible to use these techniques to identify the determinants of conformationally dependent papillomavirus-neutralizing epitopes without the aid of crystallography.

Materials and Methods

BPV1 virions, obtained from bovine warts (a gift from Carl Olson, University of Wisconsin), were isolated as described (Trus *et al*., 1997). Monoclonal antibodies 5B6 and 9 were affinity purified on Protein A–Sepharose columns and dialyzed into PBS (Roden *et al*., 1994). BPV1 virion preparations (~10 μg in PBS) were incubated at ambient temperature with a tenfold molar excess of antibody molecules, as determined by the ratio of immunoglobulin molecules to L1 total protein, in 200 μl; final volume. Immunocomplexes were collected by centrifugation in an Eppendorf bench-top centrifuge (five minutes, ambient temperature, 14,000 rpm), resuspended in 10 μl of PBS, placed on carbon-coated 400 mesh copper grids and prepared for cryo-electron microscopy as described (Booy *et al*., 1991, 1997). Samples were imaged in a Philips EM400RT electron microscope operating at 100 kV at 36,000 to 60,000 × magnification employing a modified, type 626, Gatan cooling stage and modified Gatan anti-contamination blades. Appropriate micrographs were selected, processed and reconstructed (Trus *et al*., 1997). Approximately two-thirds of the selected capsid images were used in the 3D reconstructions. Resolution was determined by both FRC3D (Conway *et al*., 1993) and SSNR3D (Unser *et al*., 1996) methods. Figures 2 3, 5 and 7 are visualized at 3.685 Å/pixel. Figure 4 is visualized at 1.84 Å/pixel. The threshold for surface shading is 120% of mass, assuming 0.78 Da/$Å^{-3}$.

Acknowledgments

We thank Carl Olson for the generous gift of bovine papillomavirus and Darren Henderson, David Belnap and James Conway for technical assistance, and we thank Alasdair Steven, Douglas Lowy and Robert Martino for encouragement and advice.

References

Baker, T. S. & Cheng, R. H. (1996). A model-based approach for determining orientations of biological macromolecules imaged by cryoelectron microscopy. *J. Struct. Biol.* **116**, 120–130.

Baker, T. S., Drak, J. & Bina, M. (1988). Reconstruction of three-dimensional structure of simian virus 40 and visualization of the chromatin core. *Proc. Natl Acad. Sci. USA,* **85**, 422–426.

Baker, T. S., Newcomb, W. W., Olson, N. H., Cowsert, L. M., Olson, C. & Brown, J. C. (1991). Structures of bovine and human papillomaviruses. Analysis by cryoelectron and three-dimensional image reconstruction. *Biophys. J.* **60**, 1445–1456.

Belnap, D. M., Olson, N. H., Cladel, N. M., Newcomb, W. W., Brown, J. C., Kreider, J. W., Christensen, N. D. & Baker, T. S. (1996). Conserved features in papillomavirus and polyomavirus capsids. *J. Mol. Biol.* **259**, 249–263.

Booy, F. P., Newcomb, W. W., Trus, B. L., Brown, J. C., Baker, T. S. & Steven, A. C. (1991). Liquid-crystalline, phage-like, packing of encapsidated DNA in herpes simplex virus. *Cell,* **64**, 1007–1015.

Booy, F. P., Trus, B. L., Davison, A. J. & Steven, A. C. (1996). The capsid architecture of Channel Catfish Virus, an evolutionarily distant herpesvirus, is largely conserved in the absence of discernible sequence homology with Herpes Simplex Virus. *Virology,* **215**, 134–141.

Böttcher, B., Wynne, S. A. & Crowther, R. A. (1997). Determination of the fold of the core protein of hepatitis B virus by cryo-electron microscopy. *Nature,* **386**, 88–91.

Breitburd, F., Kirnbauer, R., Hubbert, N. L., Nonnenmacher, B., Trin-Dinh-Desmarquet, C., Orth, G., Schiller, J. T. & Lowy, D. R. (1995). Immunization with virus-like particles from cottontail rabbit papillomavirus (CRPV) can protect against experimental CRPV infection. *J. Virol.* **69**, 3959–3963.

Christensen, N. D. & Kreider, J. W. (1990). Antibody mediated neutralization *in vivo* of infectious papillomaviruses. *J. Virol.* **64**, 3151–3156.

Christensen, N. D. & Kreider, J. W. (1991). Neutralization of CRPV infectivity by monoclonal antibodies that identify conformational epitopes on intact virions. *Virus Res.* **21(3)**, 169–179.

Christensen, N. D. & Kreider, J. W. (1993). Monoclonal antibody neutralization of BPV-1. *Virus Res,* **28**, 195–202.

Christensen, N. D., Kreider, J. W., Cladel, N. M., Patrick, S. D. & Welsh, P. A. (1990). Monoclonal antibody mediated neutralization of infectious human papillomavirus type 11. *J. Virol.* **64**, 5678–5681.

Christensen, N. D., Cladel, N. M. & Reed, C. A. (1995). Postattachment neutralization of papillomaviruses by monoclonal and polyclonal antibodies. *Virology,* **207**, 136–142.

Colonno, R. J., Callahan, P. L., Leippe, D. M., Ruekert, R. R. & Tomassini, J. E. (1989). Inhibition of rhinovirus attachment by neutralizing monoclonal antibodies and their fragments. *J. Virol.* **63**, 36–42.

Conway, J. F., Trus, B. L., Booy, F. P., Newcomb, W. W., Brown, J. C. & Steven, A. C. (1993). The effects of radiation damage on the structure of frozen hydrated HSV-1 capsids. *J. Struct. Biol.* **111**, 222–233.

Conway, J. F., Cheng, N., Zlotnick, A., Wingfield, P. T., Stahl, S. J. & Steven, A. C. (1997). Visualization of a 4-helix bundle in the hepatitis B virus capsid by cryo-electron microscopy. *Nature,* **386**, 91–94.

Crowther, R. A. (1971). Procedures for three-dimensional reconstruction of spherical viruses by Fourier synthesis from electron micrographs. *Phil. Trans. Roy. Soc. Lond. B,* **261**, 221–230.

Emini, E. A., Ostapchuk, P. & Wimmer, E. (1983). Bivalent attachment of antibody onto poliovirus leads to conformational alteration and neutralization. *J. Virol.* **48**, 547–550.

Evander, M., Frazer, I. H., Payne, E., Qi, Y. M., Hengst, K. & McMillan, N. A. J. (1997). Identification of the α6 integrin as a candidate receptor for papillomaviruses. *J. Virol.* **71**, 2449–2456.

Feng, Y., Broder, C. C., Kennedy, P. E. & Berger, E. A. (1996). HIV-1 entry co-factor: functional cDNA cloning of a seven-transmembrane domain, G-protein coupled receptor. *Science,* **272**, 872–877.

Fuller, S. D. (1987). The T = 4 envelope of Sindbis Virus is organized by interactions with a complementary T = 3 capsid. *Cell,* **48**, 923–934.

Hagensee, M. & Galloway, D. (1993). Growing human papillomaviruses and virus-like particles in the laboratory. *Papillomavirus Rep.* **4**, 121–124.

Hagensee, M. E., Olson, N. H., Baker, T. S. & Galloway, D. A. (1994). Three-dimensional structure of vaccinia virus-produced human papillomavirus type 1 capsids. *J. Virol.* **68(7)**, 4503–4505.

Hewat, E. A. & Blaas, D. (1996). Structure of a neutralizing antibody bound bivalently to human rhinovirus 2. *EMBO J.* **15**, 1515–1523.

International Agency for Research on Cancer (1995). *Human Papillomaviruses. IARC Monographs on the Evaluation of Carcinogenic Risks to Humans* (IARC working group, ed.), vol. 64, IARC Press, Lyon.

Kirnbauer, R., Booy, F., Cheng, N., Lowy, D. R. & Schiller, J. T. (1992). Papillomavirus L1 major capsid protein self-assemblies into virus-like particles that are highly immunogenic. *Proc. Natl Acad. Sci. USA,* **89(24)**, 12180–12184.

Kirnbauer, R., Chandrachud, L., O'Neil, B., Wagner, E., Grindlay, G., Armstrong, A., McGarvie, G., Schiller, J., Lowy, D. & Campo, M. (1996). Virus-like particles of Bovine Papillomavirus type 4 in prophylactic and therapeutic immunization. *Virology,* **219**, 37–44.

Liu, H., Smith, T. J., Lee, W.-M., Mosser, A. G., Ruekert, R. R., Olson, N. H., Cheng, R. H. & Baker, T. S. (1994). Structure determination of an Fab fragment that neutralizes human rhinovirus 14 and analysis of the Fab-virus complex. *J. Mol. Biol.* **240**, 127–137.

Lowy, D. R., Kirnbauer, R. & Schiller, J. T. (1994). Genital human papillomavirus infection. *Proc. Natl Acad. Sci. USA,* **91(7)**, 2436–2440.

Montgomery, R. I., Warner, M. S., Lum, B. J. & Spear, P. S. (1996). Herpes Simplex Virus-1 entry into cells mediated by a novel member of the TNF/NGF receptor family. *Cell,* **87**, 427–436.

Mosser, A. G., Leippe, D. M. & Rueckert, R. R. (1989). Neutralization of picornaviruses. In *Molecular Aspects of Picornavirus Infection and Detection* (Semler, B. L. & Ehrenfeld, E., eds), pp. 155–167, American Society for Microbiology, Washington, DC.

Olson, N. H., Kolatkar, P. R., Oliveira, M. A., Cheng, R. H., Greve, J. M., McClelland, A., Baker, T. S. & Rossmann, M. G. (1993). Structure of a human rhinovirus complexed with its receptor molecule. *Proc. Natl Acad. Sci. USA,* **90**, 507–511.

Outlaw, M. C. & Dimmock, N. J. (1991). Insights into neutralization of animal viruses gained from study of influenza virus. *Epidemiol. Infect.* **106**, 205–220.

Pfister, H. (1987). Papillomaviruses: general description, taxonomy, and classification. In *Papovaviridae: Volume 2. The Papillomaviruses* (Salzman, N. P. & Howley, P. M., eds), pp. 1–38, Plenum Press, New York.

Roden, R. B. S., Weissinger, E. M., Henderson, D. W., Booy, F., Kirnbauer, R., Mushinski, J. F., Lowy, D. R. & Schiller, J. T. (1994). Neutralization of bovine papillomavirus by antibodies to L1 and L2 capsid proteins. *J. Virol.* **68**, **(11)**, 7570–7574.

Roden, R. B. S., Hubbert, N. L., Kirnbauer, R., Breitburd, F., Lowy, D. R. & Schiller, J. T. (1995). Papillomavirus L1 capsids agglutinate mouse erythrocytes through a proteinaceous receptor. *J. Virol.* **69**, 5147–5151.

Roden, R. B. S., Hubbert, N. L., Kirnbauer, R., Christensen, N. D., Lowy, D. R. & Schiller, J. T. (1996). Assessment of the serological relatedness of genital human papillomaviruses by hemagglutination inhibition. *J. Virol.* **70**, 3298–3301.

Rossmann, M. G., Arnold, E., Erickson, J. W., Frankenberger, E. A., Griffith, J. P., Hecht, H. J., Johnson, J. E., Kamer, G., Luo, M. & Mosser, A. G. (1985). Structure of a human common cold virus and functional relationship to other picornaviruses. *Nature,* **317**, 145–153.

Schiller, J. T. & Okun, M. (1996). Papillomavirus vaccines: current status and future prospects. *Advan. Dermatol.* **11**, 355–380.

Schiller, J. T. & Roden, R. B. S. (1996). Papillomavirus-like particles: basic and applied studies. In *Papillomavirus Reviews: Current Research on Papillomaviruses* (Lacey, C., ed.), pp. 101–112, Leeds Medical Information, Leeds, UK.

Smith, T. J., Olson, N. H., Cheng, H., Chase, E. S. & Baker, T. M. (1993a). Structure of a human rhinovirus-bivalently bound antibody complex: implications for viral neutralization and antibody flexibility. *Proc. Natl Acad. Sci. USA,* **90**, 7015–7018.

Smith, T. J., Olson, N. H., Cheng, R. H., Liu, H., Chase, E., Lee, W. M., Leippe, D. M., Mosser, A. G., Ruekert, R. R. & Baker, T. M. (1993b). Structure of human rhinovirus complexed with Fab fragments from a neutralizing antibody. *J. Virol.* **67**, 1148–1158.

Stehle, T., Yan, Y., Benjamin, T. & Harrison, S. (1994). Structure of murine polyomavirus complexed with an oligosaccharide receptor fragment. *Nature,* **369**, 160–163.

Suzich, J. A., Ghim, S., Palmer-Hill, F. J., White, W. I., Tamura, J. K., Bell, J., Newsome, J. A., Jenson, A. B. & Schlegel, R. (1995). Systematic immunization with papillomavirus L1 protein completely prevents the development of viral mucosal papillomas. *Proc. Natl Acad. Sci. USA,* **92**, 11553–11557.

Thouvenin, E., Laurent, S., Madelaine, M.-F., Rasschaert, D., Vautherot, J.-F. & Hewat, E. (1997). Bivalent binding of a neutralizing antibody to a calicivirus involves torsional flexibility of the antibody hinge. *J. Mol. Biol.* **270**, 238–246.

Trus, B. L., Newcomb, W. W., Booy, F. P., Brown, J. C. & Steven, A. C. (1992). Distinct monoclonal antibodies separately label the hexons or the pentons of

herpes simplex virus capsid. *Proc. Natl Acad. Sci. USA*, **89**, 11508–11512.

Trus, B. L., Roden, R. B. S., Greenstone, H. L., Vrhel, M., Schiller, J. T. & Booy, F. P. (1997). Novel structural features of bovine papillomavirus capsid revealed by a three dimensional reconstruction to 9 Å resolution. *Nature Struct. Biol.* **4**, 413–420.

Unser, M., Vrhel, M. J., Conway, J. F., Gross, M., Thevenaz, P., Steven, A. C. & Trus, B. L. (1996). Resolution assessment of 3D reconstructions by spectral signal-to-noise ratio. In *11th EUREM*, University College, Dublin, Ireland.

Wetz, K. (1993). Attachment of neutralizing antibodies stabilizes the capsid of poliovirus against uncoating. *Virology*, **192**, 465–472.

Wickham, T. J., Mathias, P., Cheresh, D. A. & Nemerow, G. R. (1993). Integrins v3 and v5 promote adenovirus internalization but not virus attachment. *Cell*, **73**, 309–319.

Edited by W. Baumeister

(Received 23 December 1997; received in revised form 9 April 1998; accepted 29 April 1998)